Distilling from Similar Tasks for Transfer Learning on a Budget

Kenneth Borup
Aarhus University
kennethborup@math.au.dk

Cheng Perng Phoo
Cornell University
cpphoo@cs.cornell.edu

Bharath Hariharan
Cornell University
bharathh@cs.cornell.edu

Abstract

We address the challenge of getting efficient yet accurate recognition systems with limited labels. While recognition models improve with model size and amount of data, many specialized applications of computer vision have severe resource constraints both during training and inference. Transfer learning is an effective solution for training with few labels, however often at the expense of a computationally costly fine-tuning of large base models. We propose to mitigate this unpleasant trade-off between compute and accuracy via semi-supervised cross-domain distillation from a set of diverse source models. Initially, we show how to use task similarity metrics to select a single suitable source model to distill from, and that a good selection process is imperative for good downstream performance of a target model. We dub this approach DISTILLNEAREST. Though effective, DISTILLNEAREST assumes a single source model matches the target task, which is not always the case. To alleviate this, we propose a weighted multi-source distillation method to distill multiple source models trained on different domains weighted by their relevance for the target task into a single efficient model (named DISTILLWEIGHTED). Our methods need no access to source data, and merely need features and pseudo-labels of the source models. When the goal is accurate recognition under computational constraints, both DISTILLNEAREST and DISTILLWEIGHTED approaches outperform both transfer learning from strong ImageNet initializations as well as state-of-the-art semi-supervised techniques such as FixMatch. Averaged over 8 diverse target tasks our multi-source method outperforms the baselines by 5.6%-points and 4.5%-points, respectively.

1 Introduction

Recognition models get more accurate the larger they are and the more data they are trained on [22, 37, 47]. This is a problem for many applications of interest in medicine (e.g. X-ray analysis) or science (e.g. satellite-image analysis) where both labeled training data, as well as computational resources needed to train such large models, are lacking.

The challenge of limited labeled data can potentially be alleviated by fine-tuning large-scale "foundation models" [13, 22, 47]. However, fine-tuning is computationally expensive, especially when one looks at foundation models with billions of parameters [13]. Unfortunately, all evidence suggests that larger foundation models perform better at fine-tuning [22, 47]. This leaves downstream applications the unpleasant trade-off of expensive computational hardware for fine-tuning large models, or inaccu-
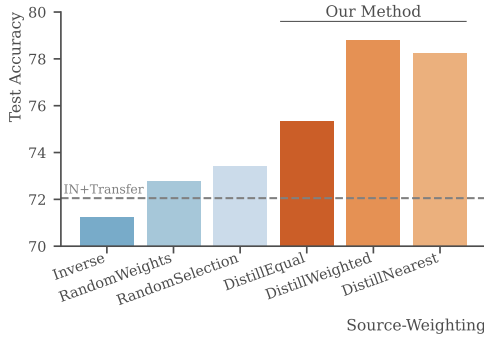
Figure 1: Average test accuracy over five target tasks with different methods for weighting source models for distillation. Our methods outperform the baselines and transfer learning from ImageNet. See Section 5.3 for details.
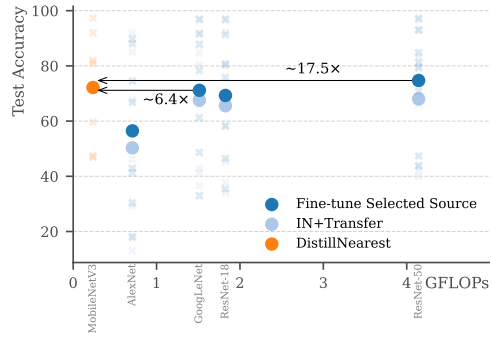

Figure 2: Average test accuracy over the 8 target tasks vs. compute requirements for a single forward pass at inference. Using DISTILLNEAREST with an efficient target architecture outperforms (or is comparable to) fine-tuning larger models.

rate results from smaller models. Motivated by this challenge, we ask *can we train accurate models on tight data and compute budgets without fine-tuning large foundation models?*

To set the scene, we assume the existence of a diverse set (both in architecture and task) of pre-trained source models (or foundation models). We do not have the resources to fine-tune these models, but we assume we can perform inference on these models and extract features, *e.g.* through APIs on cloud services [8, 35]. For the target task, we assume that labeled data is very limited, but unlabeled data is available. We then propose a simple and effective strategy for building an accurate model for the target task: DISTILLNEAREST. Concretely, we first compute a measure of "task similarity" between our target task and each source model and rank the source models accordingly. Then we pseudo-label the unlabeled data using the most similar source model. These pseudo-labels may not even be in the same label space as the target task, but we conjecture that due to the similarity between the source and target tasks, the pseudo-labels will still *group* the target data points in a task-relevant manner. Finally, we train the target model using the pseudo-labels and the available ground truth labeled data. This allows us to bypass the large computations required to fine-tune source models and directly work on the target model. At the same time, we get to effectively use the knowledge of the large source model even if it is trained on a different task.

DISTILLNEAREST assumes that a *single* best source model exists. But for some target tasks, we might need to combine multiple source models to achieve a sufficiently diverse representation to distill. We, therefore, propose an extension of our approach that distills *multiple (diverse) source models* trained on different domains, weighted by their relevance for the target task. This extension obtains even further improvements on our target performance (see Figure 1). We dub this method DISTILLWEIGHTED.

We summarize our contributions as follows:

- We train more than 200 models across a diverse set of source and target tasks using single-source distillation, and extensively show that the choice of source model is imperative for the predictive performance of the target model. To the best of our knowledge, no previous work has addressed how to efficiently select a teacher model for (cross-domain) distillation.

- We find that *task similarity metrics* correlate well with predictive performance and can be used to efficiently select and weight source models for single- and multi-source distillation without access to any source data.

- We show that our approaches yield the best accuracy on multiple target tasks under compute and data constraints. We compare our DISTILLNEAREST and DISTILLWEIGHTED methods to two baselines (transfer learning and FixMatch), as well as the naïve case of DISTILLWEIGHTED with *equal* weighting (called DISTILLEQUAL), among others. Averaged over 8 diverse datasets, our DISTILLWEIGHTED outperforms the baselines with at least 4.5% and in particular 17.5% on CUB200.
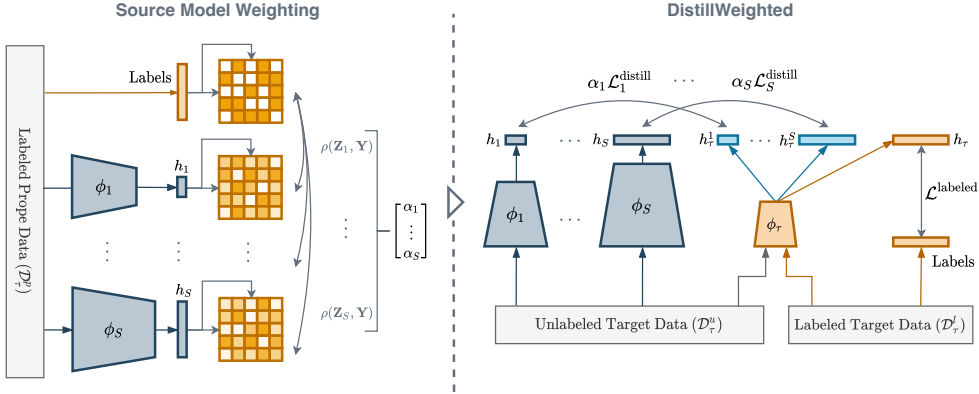
2

Figure 3: We propose to weigh a set of S source models, $\mathcal{M}_s = h_s \circ \phi_s$, by using task similarity metrics to estimate the alignment of each source model with the particular target task using a small probe set of labeled data, $\mathcal{D}_\tau^p$. Since the task similarity metrics are independent of feature dimension, we can utilize source models of any architecture and from any source task. We show that by choosing the weighting, $\alpha_1, \ldots, \alpha_S$, this way we are able to improve performance over transfer from ImageNet and training with FixMatch amongst others (see *e.g.* Table 1 and Figure 4).

2   Related Work

Knowledge Distillation One key aspect of our problem is to figure out how to compress single or multiple large foundation models into an efficient target model. A common approach is knowledge distillation [5, 18] where an efficient student model is trained to mimic the output of a larger teacher model. However, most single-teacher [3, 10, 11, 28, 30] or multi-teacher knowledge distillation [16, 27, 38, 45] research focuses on the closed set setup, where the teacher(s) and the student both attempts to tackle the same task. To the best of our knowledge, compressing models specializing in various tasks different from the target task has rarely been explored in the literature. Our paper explores this setup and illustrates that carefully distilling source models trained on different tasks can bring forth efficient yet accurate models.

Semi-Supervised Learning and Transfer Given our target tasks are specified in a semi-supervised setting, it is customary to review methods for semi-supervised learning (SSL). The key to SSL approaches is how to effectively propagate label information from a small labeled dataset to a large unlabeled dataset. Along this vein, methods such as pseudo-labeling/self-training [25, 43] or consistency regularization [7, 36, 39] have shown remarkable results in reducing deep networks dependencies on large labeled datasets via unlabeled data. However, most SSL approaches focus on training models from scratch without considering the availability of pre-trained models. Given the increasing availability of large pre-trained models [31, 42], recent work has started exploring the intersection between transfer learning and SSL [1, 20, 34]. However, most of these works focus on how to transfer from a single pre-trained model to the target task. Our paper, however, explores an even more practical setup: how to transfer from multiple pre-trained models to a downstream task where in-domain unlabeled data are available. In principle, we could combine our approach with a lot of previous work on SSL to (potentially) gain even larger improvements, but to keep our method simple we leave such exploration to future work and focus on how to better utilize an available set of pre-trained models.

Multi-Source Domain Adaptation Our setup also bears a resemblance with multi-source domain adaptation (MSDA) [32] in which the goal is to create a target model by leveraging multiple source models. However, MSDA methods often assume the source and target models share the same label space to perform domain alignment. We do not make such an assumption and in fact, focus on the case where the label space of source and target tasks have minimal to no overlap. Besides, a lot of the MSDA approaches [32, 44, 48, 49] rely on the availability of source data or the fact that the source and target tasks share the same model architecture to build domain invariant features. Given the discrepancy in assumptions between MSDA and our setup, we do not consider any methods from this line of work as baselines.
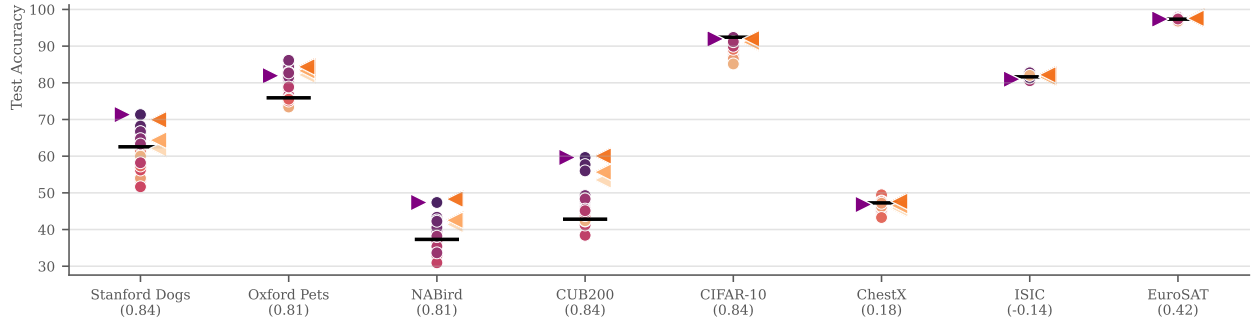
Figure 4: Test accuracy for distillation with each dot representing single-source distillation from different source models. The colors represent the task similarity for the source models (from small to large; ▬). We include the performance from fine-tuning ImageNet (▬), DISTILLNEAREST; i.e. distillation of the highest ranked source model (▶) as well as DISTILLEQUAL (◀), and DISTILL-WEIGHTED(p) where weights are proportional to task similarity with power $p = 1$ (◀), and $p = 12$ (◀), respectively. The numbers in parentheses at the bottom are Spearman correlations between the task similarity and test accuracy for single-source distillation.

Transfer Learning From Multiple Sources Transfer learning from multiple different pre-trained models has been explored in different setups. Bolya et al. [9] focuses on how to select a single good pre-trained model to use as a model initialization whereas we explore how to distill an efficient model from the pre-trained models (i.e. our target architecture could be different from those of the source models). Agostinelli et al. [4] focuses on how to select a subset of pre-trained models to construct an (fine-tuned) ensemble, whereas we focus on creating a single model. Li et al. [26] focuses on creating a generalist representation by equally distilling multiple pre-trained models using proxy/source data (which often requires high-capacity models) whereas our goal is to construct an efficient specialist model using the target data. All these works have indicated the importance of exploring how to best leverage a large collection of pre-trained models but due to differences in setup and assumptions, we do not (and could not) compare to them.

Task Similarity / Transferability Metrics A key insight of our approach is to leverage the similarity between the target and source tasks to compare and weigh different pre-trained source models during distillation. Characterizing tasks (or similarities between tasks) is an open research question with various successes. A common approach is to embed tasks into a common vector space and characterize similarities in said space. Representative research along this line of work include Achille et al. [2], Peng et al. [33], Wallace et al. [41]. Another related line of work investigates transferability metrics [6, 9, 14, 15, 29, 40]. After all, one of the biggest use cases of task similarities is to predict how well a model transfers to new tasks. Since it is not our intention to define new task similarity/transferability metrics for distillation, we use already established metrics that capture the similarity between source representations and one-hot labels to weigh the source models. Under this purview, metrics that characterize similarities between features such as CKA [12, 23] and transferability metrics based on features [9, 14] suffice.

3 Problem Setting

The aim of this paper is to train an accurate model for a given target task, subject to limited labeled data and computational constraints (*e.g.* limited compute resources). Formally, we assume that our target task is specified via a small labeled training set D_τ^l. Furthermore, we assume (a) the availability of a set of unlabeled data, D_τ^u, associated with the target task, and (b) the ability to perform inference on a set $\mathcal{S} = \{\mathcal{M}_s\}_{s=1}^S$ of S different *source* models, $\mathcal{M}_s$, trained on various source tasks different from the target task, We emphasize that we have no access to any source data which could be practical due to storage, privacy, and computational constraints. Neither do we need full access to the source models provided we can perform inference on the models anywise (*e.g.* through an API).

We assume that the architecture of the target model, $\mathcal{M}_\tau$, must be chosen to meet any applicable computational constraints. This can imply that no suitable target architecture is available in the set of

source models $\mathcal{S}$, making classical transfer learning impossible. For simplicity, we restrict our models (regardless of source or target) to classification models that can be parameterized as $\mathcal{M} = h \circ \phi$; the feature extractor ϕ embeds input $\mathbf{x}$ into a feature representation, and the classifier head, h, maps the feature $\phi(\mathbf{x})$ into predicted conditional class probabilities, $P(\mathbf{y} \mid \mathbf{x})$.

4 Cross-Task Distillation for Constructing Efficient Models from Foundation Models

To construct an efficient model, we propose to distill large foundation models. Along this vein, we propose two variants: (a) DISTILLNEAREST that distills the single nearest source model (Section 4.1) and (b) DISTILLWEIGHTED that distills a weighted collection of source models (Section 4.2).

4.1 DISTILLNEAREST

To construct a single efficient target model, DISTILLNEAREST undergoes two steps sequentially: (a) selecting an appropriate source model and (b) distilling the knowledge from the selected source model into the target model. For ease of exposition, we start by explaining the distillation process and then discuss how to select an appropriate source model.

Distilling a selected source model. Given a selected source model $\mathcal{M}_s$, the target model $\mathcal{M}_\tau = h_\tau \circ \phi_\tau$ is trained by minimizing a weighted sum of two loss functions,

$$\mathcal{L}_{\text{single}} \stackrel{\text{def}}{=} \lambda \mathcal{L}^{\text{labeled}} + (1 - \lambda)\mathcal{L}_s^{\text{distill}}, \tag{1}$$

where $\lambda \in [0, 1]$. The first loss function is the standard supervised objective over the labeled data,

$$\mathcal{L}^{\text{labeled}} \stackrel{\text{def}}{=} \frac{1}{|\mathcal{D}_\tau^l|} \sum_{(\mathbf{x}_i, \mathbf{y}_i) \in \mathcal{D}_\tau^l} \ell_{CE}\left(h_\tau(\phi_\tau(\mathbf{x}_i)), \mathbf{y}_i\right), \tag{2}$$

where $\ell_{CE}(\cdot, \cdot)$ is the cross-entropy loss. The second loss function is a distillation loss over the unlabeled data,

$$\mathcal{L}_s^{\text{distill}} \stackrel{\text{def}}{=} \frac{1}{|\mathcal{D}_\tau^u|} \sum_{\mathbf{x}_i \in \mathcal{D}_\tau^u} \ell_{CE}\left(h_\tau^s(\phi_\tau(\mathbf{x}_i)), \mathcal{M}_s(\mathbf{x}_i)\right). \tag{3}$$

Note, the source and target tasks do not share the same label space so we introduce an additional classifier head, h_τ^s, which maps the features from the target task feature extractor, ϕ_τ, to the label space of the source task. This additional classifier head, h_τ^s, is discarded after training and only the target classifier head, h_τ, is used for inference.

In principle, we could add additional semi-supervised losses, such as the FixMatch loss [36] to propagate label information from the labeled set to the unlabeled set for better performance, but this would add additional hyperparameters and entangle the effect of our methods. We leave such explorations to future work.

Selecting the nearest source model for distillation. Selecting a source model for distillation is an under-explored problem. Given the recent success of using task similarity metrics [9] for selecting foundation models for fine-tuning, we conjecture that high similarities between a source model and the target task could indicate better performance of the distilled model (we verify this in Section 5.2). However, quantifying similarities between tasks/models is an open research question with various successes [2, 29]. For simplicity, we pick our similarity based on one simple intuition: target examples with identical labels should have similar source representations and vice versa. Along this vein, the recently introduced metric, PARC [9] fits the bill.

For convenience, we briefly review PARC. Given a small labeled probe set $\mathcal{D}_\tau^p = \{(\mathbf{x}_i, \mathbf{y}_i)\}_{i=1}^n \subseteq \mathcal{D}_\tau^l$ and a source representation of interest ϕ_s, PARC first constructs two distance matrices D_{ϕ_s}, D_Y based on the Pearson correlations between every pair of examples in the probe set;

$$D_{\phi_s} = 1 - \text{pearson}(\{\phi_s(\mathbf{x}_i)\}_{i=1}^n),$$
$$D_Y = 1 - \text{pearson}(\{\mathbf{y}_i\}_{i=1}^n).$$

		Target Data		CIFAR-10	CUB200	ChestX	EuroSAT	ISIC	NABird	Oxford Pets	Stanford Dogs	Mean
		Labeled	Unlabeled									
MobileNetV3 (0.24 GFLOPs)	IN+Transfer	✓	-	<u>92.4</u>	42.8	<u>47.3</u>	97.4	81.6	37.3	75.9	62.6	67.2
	IN+FixMatch	✓	✓	**93.5**	41.9	38.5	**98.1**	**82.6**	*42.8*	<u>83.4</u>	*65.8*	68.3
	DISTILLRANDOMSELECTION	✓	✓	89.6	46.5	46.6	97.4	*81.8*	39.0	79.4	61.9	67.8
	(Ours) DISTILLNEAREST	✓	✓	92.0	<u>59.6</u>	46.8	97.4	81.0	<u>47.4</u>	81.9	**71.3**	<u>72.2</u>
	DISTILLEQUAL	✓	✓	90.8	*53.5*	45.7	97.5	81.5	41.4	*82.1*	62.1	*69.3*
	DISTILLRANDOMWEIGHTS	✓	✓	87.9	44.9	*46.9*	<u>97.8</u>	81.6	39.6	80.2	59.2	67.3
	(Ours) DISTILLWEIGHTED	✓	✓	*92.0*	**60.0**	**47.7**	97.6	<u>82.2</u>	**48.3**	**84.4**	<u>69.9</u>	**72.8**
AlexNet (0.71 GFLOPs)	IN+Transfer	✓	-	85.0	18.4	46.2	91.9	67.8	13.0	50.9	29.1	50.3
	Fine-tune Selected Source	✓	-	88.0	30.4	42.9	89.8	74.5	17.9	66.8	41.3	56.5
GoogLeNet (1.51 GFLOPs)	IN+Transfer	✓	-	91.8	42.8	41.4	96.8	80.5	36.5	84.8	65.9	67.6
	Fine-tune Selected Source	✓	-	91.6	61.2	48.6	96.9	78.3	33.0	87.8	71.8	71.2
ResNet-18 (1.83 GFLOPs)	IN+Transfer	✓	-	92.2	37.8	45.2	96.6	80.2	34.0	80.2	58.2	65.6
	Fine-tune Selected Source	✓	-	91.3	58.2	46.4	97.0	75.8	35.4	80.7	69.3	69.3
ResNet-50 (4.14 GFLOPs)	IN+Transfer	✓	-	92.9	42.0	43.4	96.8	79.9	39.9	83.3	65.9	68.0
	Fine-tune Selected Source	✓	-	93.0	70.8	43.9	97.2	81.3	47.4	84.8	79.3	74.7

Table 1: Cross-task distillation compared to baselines. MobileNetV3 models (target architecture) trained with our methods are highly competitive with baseline methods on MobileNetV3 as well as baseline methods for more demanding model architectures (source architectures: Alexnet, GoogLeNet, ResNet-18, ResNet-50). We highlight the top 3 methods, which comply with compute requirements (i.e. MobileNetV3) for each target task by **bold**, <u>underline</u>, and *italic*, respectively. We also indicate the target data used by different methods.

PARC is computed as the Spearman correlation between the lower triangles of the distance matrices;

$$\text{PARC}(\phi_s, Y) = \text{spear}\left(\{D_{\phi_s}[i,j]\}_{i<j}, \{D_Y[i,j]\}_{i<j}\right).$$

Intuitively, PARC quantifies the similarity of representations by comparing the (dis)similarity structures of examples within different feature spaces: if two representations are similar, then (dis)similar examples in one feature space should stay (dis)similar in the other feature space. In Figure 4 and 5 we show that ranking source models by PARC correlates well with test accuracy and that selecting an appropriate source model can yield significant improvements.

4.2 DISTILLWEIGHTED

Above, DISTILLNEAREST assumes a single optimal source model exists for the target task, but what if no single source model aligns well with our target task? To alleviate this issue, we propose to distill multiple source models, weighted according to their similarities with the target tasks. In the following, we explain our weighted distillation objective and how the weights are constructed. Figure 3 is a schematic depiction of the approach DISTILLWEIGHTED.

Weighted objective for distilling multiple sources. Given a set of source models $\mathcal{S} = \{M_s\}_{s=1}^{S}$, we modify the distillation loss of (1) with a weighted sum of multiple distillation losses (one for each source model):

$$\mathcal{L}_{\text{multi}} \stackrel{\text{def}}{=} \lambda \mathcal{L}^{\text{labeled}} + (1-\lambda) \sum_{s=1}^{S} \alpha_s \mathcal{L}_s^{\text{distill}}, \tag{4}$$

where $\lambda, \alpha_1, \ldots, \alpha_S \in [0,1]$ ($\mathcal{L}^{\text{labeled}}$ and $\mathcal{L}_s^{\text{distill}}$ are as defined in (2) and (3), respectively). Here α_s is the relative weight assigned to each source model such that $\sum_{s=1}^{S} \alpha_s = 1$. Once again, we could add additional semi-supervised losses, such as the FixMatch loss, but to ensure simplicity, we leave such explorations for future research.

Task similarity weighting of source models Simply assigning equal weight to all source models is sub-optimal (e.g. weighing source models trained on ImageNet and Chest X-ray equally might not be optimal for recognizing birds). As such, we propose to compute the source weight α_s from a task

similarity metric between the s-th source model and the target task. In particular, let e_s be such a similarity metric, then we compute the source weights $\{\alpha_i\}_{i\in[S]}$ as

$$\alpha_i = \frac{\underline{e}_i^p}{\sum_{s=1}^{S} \underline{e}_s^p}, \quad \text{where } \underline{e}_j = \max(0, e_j) \tag{5}$$

for $j = 1, \ldots, S$. Here p is a hyperparameter to re-scale the distribution of the weights. Larger p assigns more weight to the most similar source models, while $p = 0$ corresponds to equal weights for all models (denoted DISTILLEQUAL), and $p \to \infty$ assigns all weight to the most similar source model (i.e. DISTILLNEAREST). When relevant, we use the notation DISTILLWEIGHTED(p) to indicate the choice of p.

Scalability For DISTILLWEIGHTED to be feasible, compared to DISTILLNEAREST, we need to ensure that the training procedure scales well with the size of $\mathcal{S}$. Since the computation of the weights $\{\alpha_s\}_{s=1}^{S}$ is based on the small probe set and is almost identical to the selection procedure for DISTILLNEAREST this is a negligible step. When training the target model, we merely require one forward pass on the unlabeled target dataset with each source model (to obtain pseudo-labels) as well as training of a one-layer classifier head per source model, both of which are cheap compared to the full training procedure of the target model. Nonetheless, one could employ a pre-selection of the top-k source models with the largest task similarity, thereby reducing the number of classifier heads and forward passes required. However, doing so introduces another hyperparameter, k, (i.e. how many models to use) complicating the analysis. Moreover, since large p induces such pre-selection in a *soft* manner, we leave it to future research to determine how to select the appropriate k.

5 Experiments and Results

5.1 Experimental Setup

Benchmark. Despite our methods being designed with the interest of using large vision models (that are potentially only available for inference), such a setting is intractable for our research. Thus, to allow for controlled experimentation we restrict our source models to a more tractable scale. In particular, we modify an existing transfer learning benchmark: Scalable Diverse Model Selection by [9], and use the publicly available models to construct a set of source models for each target task. Thus, we consider a set consisting of 28 models: 4 architectures (AlexNet, GoogLeNet, ResNet-18, and ResNet-50 [17, 24]) trained on 7 different source tasks (CIFAR-10, Caltech101, CUB200, NABird, Oxford Pets, Stanford Dogs, and VOC2007). For the target tasks, we consider 8 different tasks covering various image domains (Natural images: CIFAR-10, CUB200, NABird, Oxford Pets, Stanford Dogs; X-ray: ChestX; Skin Lesion Images: ISIC; Satellite Images: EuroSAT). We carefully remove any source models associated with a particular target task, if such exists, in order to avoid information leakage between source and target tasks (see also supplementary materials for further considerations). For the target architecture, we use MobileNetV3 [19] due to its low computational requirements compared to any of the source models. We refer the reader to the supplementary material for further details on implementation.

Baselines. We consider a set of different baselines: based on ImageNet initializations we consider IN+TRANSFER (fine-tunes ImageNet representations using only the labeled data), and IN+FIXMATCH [36] (fine-tunes the ImageNet representation using labeled and unlabeled data), and based on source model initializations we fine-tune the highest-ranked source model of each source architecture. To show the importance of using the right source model(s) to distill, we also compare DISTILLNEAREST to DISTILLRANDOMSELECTION which is the average of distilling from a randomly selected source, and for comparison to DISTILLWEIGHTED we also construct distilled models using the multi-source objective (4) with a random weight (DISTILLRANDOMWEIGHTS) and equal weights (DISTILLEQUAL). For ease of exposition, we present results for DISTILLNEAREST (Section 5.2) and DISTILLWEIGHTED (Section 5.3) in separate sections.

5.2 Results for DISTILLNEAREST

We compare DISTILLNEAREST with the baselines in Table 1 and Figure 4. Our observations are as follows.

Distillation with the right source model is better than fine-tuning from ImageNet. We observe that within the same target architecture (MobileNetv3), simply fine-tuning ImageNet representations (IN+TRANSFER) is less optimal than distilling from the most similar single model (DISTILLNEAREST). In fact, for fine-grained datasets such as CUB200, NABird, Oxford Pets, and Stanford Dogs, we observe that distilling from an appropriate source model (DISTILLNEAREST) could yield much better performance than fine-tuning from a generalist ImageNet representation. More surprisingly, even with the aid of unlabeled data, models fine-tuned from ImageNet representations using a label propagation style approach (IN+FIXMATCH) still underperform distillation-based methods by at least 3.9% on average. These observations indicate the importance of selecting the right source model for transfer/distillation.

Distilling to efficient architecture could be better than fine-tuning larger models. In Table 1, we include the performance when fine-tuning larger architectures trained on ImageNet (IN+TRANSFER) and the source model (of the same architecture) most similar to each target task selected using PARC (FINE-TUNE SELECTED SOURCE). A few observations are immediate: (a) our choice of task similarity metric is effective for transfer; across all 4 architectures, we observe at least 4% improvement over simple fine-tuning from ImageNet, which validates the results by Bolya et al. [9], and (b) with the aid of unlabeled data and distillation, the computationally efficient architecture MobileNetV3 can outperform larger architectures fine-tuned on labeled data from the target task (i.e. AlexNet, GoogLeNet, ResNet-18). Although underperforming fine-tuning a ResNet-50 initialized with the most similar ResNet-50 source model by a mere average of 2.5%-points (FINE-TUNE SELECTED SOURCE), using a ResNet-50 would require $17.5\times$ more computations during inference to achieve such improvements.

5.2.1 Task Similarity Metrics for DISTILLNEAREST

One key component of DISTILLNEAREST is to select the source model to perform cross-task distillation on using task similarity metrics. Despite many many existing metrics for quantifying task similarities, their effectiveness for distillation remains unclear. Given the myriads of metrics, we restrict our focus to metrics that can capture similarities between a source representation of a target example and its one-hot label representation. Along this vein, two questions arise: which metric to use for comparing representations, and which representations from a source model should be used to represent a target example?

For the first question, we look into multiple metrics in the literature that compares various representations: CKA [12], RSA [14], and PARC [9]. For the second question, we look into the common representations from a source model: the features ϕ and the probabilistic outputs $h \circ \phi$.

To establish the effectiveness of our choice of similarity metric, we report the Spearman correlation between the task similarities and the test accuracy of the distilled models in Table 2. We see that features from the source models can better capture the correlation between the source models and the test accuracy of the distilled models, than the probabilistic pseudo-labels. In addition, we also see a much higher correlation among natural tasks (compared to specialized tasks such as ChestX, EuroSAT, and ISIC) which suggests that our choice of task similarity is effective at selecting similar tasks. Besides, we also observe a higher correlation when using PARC compared to the other metrics, thus validating our choice of using PARC as the default metric.

To further establish the effectiveness of our metrics to rank various source models, we compute the relative test accuracy between the top-3 models most similar to the target task and the top-3 best models after distillation (see Table 3). Again, we observe that all three metrics are capable of ranking affinity between source models, but ranking the models with PARC outperforms the other two metrics.

5.3 Results for DISTILLWEIGHTED

From Table 1, we observe that DISTILLWEIGHTED compares favorably to DISTILLNEAREST, thus the conclusions for DISTILLNEAREST translates to DISTILLWEIGHTED. Yet, one particular task, Oxford Pets, is worth more attention. On Oxford Pets (classification of different breeds of cats and dogs), we observe that distilling from multiple weighted sources (DISTILLWEIGHTED) is much better than distilling from the single most similar source (DISTILLNEAREST), which is a ResNet-18 trained on Caltech101 (that can recognize concepts such as Dalmatian dog, spotted cats, etc.). Although the

		CIFAR-10	CUB200	ChestX	EuroSAT	ISIC	NABird	Oxford Pets	Stanford Dogs	Mean
Pseudo	CKA	0.72	0.62	0.23	0.39	-0.04	0.31	0.69	0.11	0.38
	PARC	0.79	0.79	0.02	0.17	0.06	0.48	0.72	0.54	0.45
	RSA	0.82	0.31	-0.11	0.30	**0.10**	-0.03	0.65	0.38	0.30
Feature	CKA	0.82	0.39	**0.36**	0.21	-0.04	0.47	0.69	0.55	0.43
	PARC	0.84	**0.84**	0.18	**0.42**	-0.14	**0.81**	0.81	0.84	**0.58**
	RSA	**0.86**	0.81	0.03	0.38	0.03	0.28	**0.89**	**0.85**	0.52

Table 2: Spearman correlation between test accuracy after all possible single-source distillations and task similarities associated with the source models. Generally feature representations correlate better with distillation performance compared to pseudo-label representations.

		CIFAR-10	CUB200	ChestX	EuroSAT	ISIC	NABird	Oxford Pets	Stanford Dogs	Mean
Pseudo	CKA	99.1	95.6	97.4	99.6	98.8	89.4	**100.0**	97.6	97.2
	PARC	99.5	**100.0**	95.5	99.6	98.5	99.7	98.8	**99.7**	98.9
	RSA	**100.0**	77.7	96.5	99.7	98.5	87.2	98.6	97.6	94.5
Feature	CKA	**100.0**	95.6	97.0	**99.8**	**99.0**	93.3	**100.0**	96.4	97.6
	PARC	**100.0**	**100.0**	**97.8**	99.7	98.3	**100.0**	97.1	98.5	**98.9**
	RSA	**100.0**	**100.0**	96.7	99.8	98.9	94.9	98.9	98.8	98.5

Table 3: Relative accuracy of top-3 single-source distilled models selected by task similarity over the average of the 3 actual best models. We compute the average test accuracy of the top-3 highest ranked target models and divide it by the average of the 3 actually best-performing target models.

most similar source model contains relevant information for recognizing different breeds of dogs and cats, it might not contain all relevant knowledge from the set of source models that could be conducive to recognizing all visual concepts in Oxford Pets. In fact, we observe that the second most similar model is a GoogLeNet model trained on Stanford Dogs to recognize more dog breeds than the most similar source model (but incapable of recognizing cats). In this case, DISTILLWEIGHTED allows aggregation of knowledge from multiple sources and can effectively combine knowledge from

Figure 5: Test accuracy of single-source distillation and raw task similarity score using PARC on the feature representations. The scores are on different scales for different tasks, but almost all tasks have a positive correlation between test accuracy and task similarity.

Figure 6: Improvement over IN+TRANSFER. Here ● is the average improvement over all eight target tasks and ● represents the performance on a target task. Note, $p = 0$ corresponds to DISTILLEQUAL, and $p = \infty$ corresponds to DISTILLNEAREST.

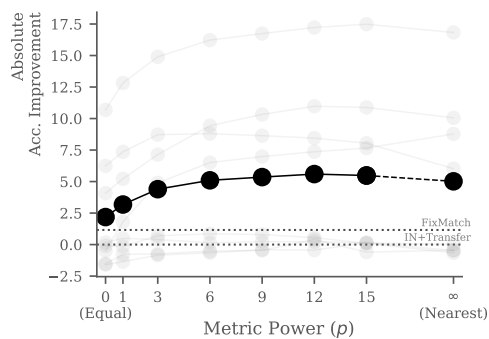different source models for a more accurate target model than distillation from a single source. This suggests that *under certain conditions such as high heterogeneity in data, distilling from multiple source models can outperform distilling a single best source model.*

5.3.1 Task Similarity Metrics for Weighing Sources

We have established that our task similarity metric can capture the correlation between the source model representations and the test accuracy of the distilled models. However, it is not a priori clear that weighing source models based on the ranking of their affinity to the target task would yield better performance for multi-source distillation. As such, we investigate alternative choices of weighing schemes for a subset of 5 target tasks (CUB200, EuroSAT, ISIC, Oxford Pets, Stanford Dogs): INVERSE (weights are inversely proportional to task similarity), DISTILLRANDOMWEIGHTS (weights are sampled uniformly on a 4-simplex), DISTILLRANDOMSELECTION (randomly selecting a single source model), and DISTILLEQUAL (equal weights for all models).

Through Figure 1, we find that distilling from a single or set of source models ranked using the similarity metric is much more effective than distilling from source models that are weighted randomly or equally (DISTILLRANDOMWEIGHTS or DISTILLEQUAL). In addition, the fact that INVERSE underperforms IN+TRANSFER on average suggests that it is crucial to follow the ranking induced by the similarity metrics when distilling the sources and that the metric ranks both the most similar source models and the least similar source models appropriately.

5.3.2 Effect of p

Our task similarity metrics give a good ranking of which source models to select for distillation but it is unclear whether the similarity score could be used directly without any post-processing. To investigate, we visualize the relationship between the test accuracy of the models distilled from a single source and our task similarity. From Figure 5, it is clear that the distribution of task similarities depends on the target task, which motivates our normalization scheme.

In addition, it is not apriori clear that the weights should scale linearly with the similarity scores. Thus, we investigate the effect of the rescaling factor, p, for constructing the weights. In Figure 6, we see that although no rescaling ($p = 1$) outperforms equal weighting, it is less optimal than *e.g.* $p = 12$ (our default). This suggests that task similarity and good weights have a monotonic, but non-linear relationship.

5.4 Additional Ablations and Analyses

Due to space constraints, we include additional ablations and analyses in the supplementary materials. We summarize the main findings as follows.

ResNet-50 as target model. Averaged over 8 tasks, DISTILLWEIGHTED outperforms both IN+TRANSFER and DISTILLEQUAL by 5.6% and 3.8%, respectively. Also, compared to ImageNet initialization, using DISTILLWEIGHTED with the most similar ResNet-50 source model as target model initialization improves accuracy by 1.0%.

Improvements on VTAB. DISTILLWEIGHTED outperforms IN+TRANSFER averaged over the ● *Natural* and ● *Specialized* tasks of VTAB, by 5.1% and 0.8%, respectively. DISTILLNEAREST outperform by 4.8% and 0.6%, respectively.

Fewer labels. DISTILLWEIGHTED and DISTILLNEAREST outperform IN+TRANSFER (by 6.8% and 4.4%, respectively) under a setup with even fewer labeled samples.

Additional analysis of task similarity metrics. We consider additional correlation metrics and top-k relative accuracies of the selected models — all supporting the usefulness of task similarity to weigh and select source models.

6 Conclusion

We investigate the use of diverse source models to obtain efficient and accurate models for visual recognition with limited labeled data. In particular, we propose to distill multiple diverse source

models from different domains weighted by their relevance to the target task without access to any source data. We show that under computational constraints and averaged over a diverse set of target tasks, our methods outperform both transfer learning from ImageNet initializations and state-of-the-art semi-supervised techniques.

References

[1] A. Abuduweili, X. Li, H. Shi, C.-Z. Xu, and D. Dou. Adaptive consistency regularization for semi-supervised transfer learning. In *Proceedings of the IEEE/CVF Conference on Computer Vision and Pattern Recognition*, pages 6923–6932, 2021. 3

[2] A. Achille, M. Lam, R. Tewari, A. Ravichandran, S. Maji, C. Fowlkes, S. Soatto, and P. Perona. Task2Vec: Task embedding for meta-learning. In *Proceedings of the IEEE International Conference on Computer Vision*, pages 6429–6438, 2019. ISBN 9781728148038. doi: 10.1109/ICCV.2019.00653. 4, 5

[3] R. Adriana, B. Nicolas, K. S. Ebrahimi, C. Antoine, G. Carlo, and B. Yoshua. Fitnets: Hints for thin deep nets. *Proc. ICLR*, 2, 2015. 3

[4] A. Agostinelli, J. Uijlings, T. Mensink, and V. Ferrari. Transferability Metrics for Selecting Source Model Ensembles. In *Proceedings of the IEEE/CVF Conference on Computer Vision and Pattern Recognition*, pages 7936–7946, 2022. URL http://arxiv.org/abs/2111.13011. 4, 18

[5] L. J. Ba and R. Caruana. Do Deep Nets Really Need to be Deep? *Advances in Neural Information Processing Systems*, 3(January):2654–2662, 2014. ISSN 10495258. 3

[6] Y. Bao, Y. Li, S.-L. Huang, L. Zhang, L. Zheng, A. Zamir, and L. Guibas. An information-theoretic approach to transferability in task transfer learning. In *2019 IEEE International Conference on Image Processing (ICIP)*, pages 2309–2313. IEEE, 2019. 4

[7] D. Berthelot, N. Carlini, I. Goodfellow, N. Papernot, A. Oliver, and C. A. Raffel. Mixmatch: A holistic approach to semi-supervised learning. *Advances in neural information processing systems*, 32, 2019. 3

[8] E. Bisong and E. Bisong. Google colaboratory. *Building machine learning and deep learning models on google cloud platform: a comprehensive guide for beginners*, pages 59–64, 2019. 2

[9] D. Bolya, R. Mittapalli, and J. Hoffman. Scalable Diverse Model Selection for Accessible Transfer Learning, 2021. ISSN 10495258. 4, 5, 7, 8, 17, 19, 20

[10] K. Borup and L. N. Andersen. Even your teacher needs guidance: Ground-truth targets dampen regularization imposed by self-distillation. *Advances in Neural Information Processing Systems*, 34:5316–5327, 2021. 3

[11] J. H. Cho and B. Hariharan. On the Efficacy of Knowledge Distillation. *ICCV*, 2019. ISSN 00262714. doi: 10.1016/0026-2714(74)90354-0. 3

[12] C. Cortes, M. Mohri, and A. Rostamizadeh. Algorithms for learning kernels based on centered alignment. *Journal of Machine Learning Research*, 13:795–828, 2012. ISSN 15324435. 4, 8, 19

[13] M. Dehghani, J. Djolonga, B. Mustafa, P. Padlewski, J. Heek, J. Gilmer, A. Steiner, M. Caron, R. Geirhos, I. Alabdulmohsin, R. Jenatton, L. Beyer, M. Tschannen, A. Arnab, X. Wang, C. Riquelme, M. Minderer, J. Puigcerver, U. Evci, M. Kumar, S. van Steenkiste, G. F. Elsayed, A. Mahendran, F. Yu, A. Oliver, F. Huot, J. Bastings, M. P. Collier, A. Gritsenko, V. Birodkar, C. Vasconcelos, Y. Tay, T. Mensink, A. Kolesnikov, F. Pavetić, D. Tran, T. Kipf, M. Lučić, X. Zhai, D. Keysers, J. Harmsen, and N. Houlsby. Scaling Vision Transformers to 22 Billion Parameters. 2023. 1

[14] K. Dwivedi and G. Roig. Representation similarity analysis for efficient task taxonomy & transfer learning. *Proceedings of the IEEE Computer Society Conference on Computer Vision and Pattern Recognition*, 2019-June:12379–12388, 2019. ISSN 10636919. doi: 10.1109/CVPR.2019.01267. 4, 8, 19

[15] K. Dwivedi, J. Huang, R. M. Cichy, and G. Roig. Duality diagram similarity: a generic framework for initialization selection in task transfer learning. In *European Conference on Computer Vision*, pages 497–513. Springer, 2020. 4

[16] T. Fukuda, M. Suzuki, G. Kurata, S. Thomas, J. Cui, and B. Ramabhadran. Efficient knowledge distillation from an ensemble of teachers. In *Interspeech*, pages 3697–3701, 2017. 3

[17] K. He, X. Zhang, S. Ren, and J. Sun. Deep residual learning for image recognition. *Proceedings of the IEEE Computer Society Conference on Computer Vision and Pattern Recognition*, 2016-Decem:770–778, 2016. ISSN 10636919. doi: 10.1109/CVPR.2016.90. 7

[18] G. Hinton, O. Vinyals, and J. Dean. Distilling the Knowledge in a Neural Network. *arXiv preprint arXiv:1503.02531*, pages 1–9, 2015. URL http://arxiv.org/abs/1503.02531. 3

[19] A. Howard, M. Sandler, G. Chu, L.-C. Chen, B. Chen, M. Tan, W. Wang, Y. Zhu, R. Pang, V. Vasudevan, and L. H. Adam1. Searching for MobileNetV3. *Proceedings of the IEEE International Conference on Computer Vision*, 2019-Octob:1314–1324, 2019. ISSN 15505499. doi: 10.1109/ICCV.2019.00140. 7

[20] A. Islam, C.-F. R. Chen, R. Panda, L. Karlinsky, R. Feris, and R. J. Radke. Dynamic Distillation Network for Cross-Domain Few-Shot Recognition with Unlabeled Data. In M. Ranzato, A. Beygelzimer, Y. Dauphin, P. S. Liang, and J. W. Vaughan, editors, *Advances in Neural Information Processing Systems*, volume 34, pages 3584–3595. Curran Associates, Inc., 2021. URL https://proceedings.neurips.cc/paper/2021/file/1d6408264d31d453d556c60fe7d0459e-Paper.pdfhttp://arxiv.org/abs/2106.07807. 3

[21] M. Jia, L. Tang, B.-C. Chen, C. Cardie, S. Belongie, B. Hariharan, and S.-N. Lim. Visual Prompt Tuning. *arXiv*, 2022. URL http://arxiv.org/abs/2203.12119. 20

[22] A. Kolesnikov, L. Beyer, X. Zhai, J. Puigcerver, J. Yung, S. Gelly, and N. Houlsby. Big Transfer (BiT): General Visual Representation Learning. *Lecture Notes in Computer Science (including subseries Lecture Notes in Artificial Intelligence and Lecture Notes in Bioinformatics)*, 12350 LNCS:491–507, 2020. ISSN 16113349. doi: 10.1007/978-3-030-58558-7{_}29. 1, 20

[23] S. Kornblith, M. Norouzi, H. Lee, and G. Hinton. Similarity of neural network representations revisited. In *International Conference on Machine Learning*, pages 3519–3529. PMLR, 2019. 4

[24] A. Krizhevsky, I. Sutskever, G. E. Hinton, S. Ilya, and G. E. Hinton. ImageNet Classification with Deep Convolutional Neural Networks. In F. Pereira, C. J. Burges, L. Bottou, and K. Q. Weinberger, editors, *Advances in Neural Information Processing Systems*, volume 25. Curran Associates, Inc., 2012. 7

[25] D.-H. Lee et al. Pseudo-label: The simple and efficient semi-supervised learning method for deep neural networks. In *Workshop on challenges in representation learning, ICML*, page 896, 2013. 3

[26] Z. Li, A. Ravichandran, C. Fowlkes, M. Polito, R. Bhotika, and S. Soatto. Representation Consolidation for Training Expert Students, 2021. URL http://arxiv.org/abs/2107.08039. 4

[27] Y. Liu, W. Zhang, and J. Wang. Adaptive multi-teacher multi-level knowledge distillation. *Neurocomputing*, 415:106–113, 2020. 3

[28] S.-I. Mirzadeh, M. Farajtabar, A. Li, H. Ghasemzadeh, N. Levine, A. Matsukawa, and H. Ghasemzadeh. Improved Knowledge Distillation via Teacher Assistant: Bridging the Gap Between Student and Teacher. *arXiv preprint arXiv:1902.03393*, 2019. URL http://arxiv.org/abs/1902.03393. 3

[29] C. Nguyen, T. Hassner, M. Seeger, and C. Archambeau. Leep: A new measure to evaluate transferability of learned representations. In *International Conference on Machine Learning*, pages 7294–7305. PMLR, 2020. 4, 5

[30] W. Park, D. Kim, Y. Lu, and M. Cho. Relational Knowledge Distillation. In *Proceedings of the IEEE Computer Society Conference on Computer Vision and Pattern Recognition*, 2019. ISBN 9781728132938. doi: 10.1109/CVPR.2019.00409. 3

[31] A. Paszke, S. Gross, F. Massa, A. Lerer, J. Bradbury, G. Chanan, T. Killeen, Z. Lin, N. Gimelshein, L. Antiga, A. Desmaison, A. Kopf, E. Yang, Z. DeVito, M. Raison, A. Tejani, S. Chilamkurthy, B. Steiner, L. Fang, J. Bai, and S. Chintala. Pytorch: An imperative style, high-performance deep learning library. In H. Wallach, H. Larochelle, A. Beygelzimer, F. d'Alché-Buc, E. Fox, and R. Garnett, editors, *Advances in Neural Information Processing Systems*, volume 32. Curran Associates, Inc., 2019. 3

[32] X. Peng, Q. Bai, X. Xia, Z. Huang, K. Saenko, and B. Wang. Moment matching for multi-source domain adaptation. In *Proceedings of the IEEE/CVF international conference on computer vision*, pages 1406–1415, 2019. 3

[33] X. Peng, Y. Li, and K. Saenko. Domain2Vec: Domain Embedding for Unsupervised Domain Adaptation. In A. Vedaldi, H. Bischof, T. Brox, and J.-M. Frahm, editors, *Computer Vision – ECCV 2020*, pages 756–774, Cham, 2020. Springer International Publishing. ISBN 978-3-030-58539-6. 4

[34] C. P. Phoo and B. Hariharan. Self-training For Few-shot Transfer Across Extreme Task Differences. In *International Conference on Learning Representations*, pages 1–19, 2021. URL http://arxiv.org/abs/2010.07734https://openreview.net/forum?id=O3Y56aqpChA. 3

[35] A. Rekognition. URL https://aws.amazon.com/rekognition/. 2

[36] K. Sohn, D. Berthelot, N. Carlini, Z. Zhang, H. Zhang, C. A. Raffel, E. D. Cubuk, A. Kurakin, C.-L. L. Li, Z. Zhang, N. Carlini, E. D. Cubuk, A. Kurakin, H. Zhang, and C. A. Raffel. FixMatch: Simplifying Semi-Supervised Learning with Consistency and Confidence. In H. Larochelle, M. Ranzato, R. Hadsell, M. F. Balcan, and H. Lin, editors, *Advances in Neural Information Processing Systems*, volume 33, pages 596–608. Curran Associates, Inc., 2020. 3, 5, 7

[37] C. Sun, A. Shrivastava, S. Singh, and A. Gupta. Revisiting unreasonable effectiveness of data in deep learning era. In *Proceedings of the IEEE international conference on computer vision*, pages 843–852, 2017. 1

[38] X. Tan, Y. Ren, D. He, T. Qin, Z. Zhao, and T.-Y. Liu. Multilingual neural machine translation with knowledge distillation. *arXiv preprint arXiv:1902.10461*, 2019. 3

[39] A. Tarvainen and H. Valpola. Mean teachers are better role models: Weight-averaged consistency targets improve semi-supervised deep learning results. *Advances in neural information processing systems*, 30, 2017. 3

[40] A. T. Tran, C. V. Nguyen, and T. Hassner. Transferability and hardness of supervised classification tasks. In *Proceedings of the IEEE/CVF International Conference on Computer Vision*, pages 1395–1405, 2019. 4

[41] B. Wallace, Z. Wu, and B. Hariharan. Can we characterize tasks without labels or features? In *Proceedings of the IEEE/CVF Conference on Computer Vision and Pattern Recognition (CVPR)*, pages 1245–1254, June 2021. 4

[42] T. Wolf, L. Debut, V. Sanh, J. Chaumond, C. Delangue, A. Moi, P. Cistac, T. Rault, R. Louf, M. Funtowicz, et al. Huggingface's transformers: State-of-the-art natural language processing. *arXiv preprint arXiv:1910.03771*, 2019. 3

[43] Q. Xie, M.-T. Luong, E. Hovy, and Q. V. Le. Self-training with noisy student improves imagenet classification. In *Proceedings of the IEEE/CVF conference on computer vision and pattern recognition*, pages 10687–10698, 2020. 3

12

[44] R. Xu, Z. Chen, W. Zuo, J. Yan, and L. Lin. Deep cocktail network: Multi-source unsupervised domain adaptation with category shift. In *Proceedings of the IEEE conference on computer vision and pattern recognition*, pages 3964–3973, 2018. 3

[45] S. You, C. Xu, C. Xu, and D. Tao. Learning from multiple teacher networks. In *Proceedings of the 23rd ACM SIGKDD International Conference on Knowledge Discovery and Data Mining*, pages 1285–1294, 2017. 3

[46] X. Zhai, J. Puigcerver, A. Kolesnikov, P. Ruyssen, C. Riquelme, M. Lucic, J. Djolonga, A. S. Pinto, M. Neumann, A. Dosovitskiy, L. Beyer, O. Bachem, M. Tschannen, M. Michalski, O. Bousquet, S. Gelly, and N. Houlsby. A Large-scale Study of Representation Learning with the Visual Task Adaptation Benchmark. *arXiv*, 2019. URL http://arxiv.org/abs/1910.04867. 14, 20

[47] X. Zhai, A. Kolesnikov, N. Houlsby, and L. Beyer. Scaling Vision Transformers. *Proceedings of the IEEE Computer Society Conference on Computer Vision and Pattern Recognition*, 2022-June:12094–12103, 2022. ISSN 10636919. doi: 10.1109/CVPR52688.2022.01179. 1

[48] H. Zhao, S. Zhang, G. Wu, J. M. Moura, J. P. Costeira, and G. J. Gordon. Adversarial multiple source domain adaptation. *Advances in neural information processing systems*, 31, 2018. 3

[49] S. Zhao, G. Wang, S. Zhang, Y. Gu, Y. Li, Z. Song, P. Xu, R. Hu, H. Chai, and K. Keutzer. Multi-source distilling domain adaptation. In *Proceedings of the AAAI Conference on Artificial Intelligence*, volume 34, pages 12975–12983, 2020. 3

A Additional Ablations and Analyses

We present additional results and implementation details in the supplementary. To avoid confusion, we use the same set of index numbers as in the main text to refer to the tables and figures. Please find Tables 1-3 and Figures 1-6 in the main text.

A.1 Results on VTAB

We report the results of our VTAB [46] experiment in Table 4. On VTAB, We find that both DISTILLWEIGHTED and DISTILLNEAREST distillation outperform IN+TRANSFER on each of the ● *Natural* tasks. Particularly, DISTILLWEIGHTED outperforms IN+TRANSFER with 13.9%-points on CIFAR-10 and 10.6%-points on Sun397 and averaged across ● *Natural* DISTILLWEIGHTED outperforms IN+TRANSFER with 5.1%-points. Average over ● *Specialized* both DISTILLWEIGHTED and DISTILLNEAREST outperform IN+TRANSFER, although with a small margin. Finally, averaged over ● *Structured* IN+TRANSFER outperforms our methods, but due to the nature of these tasks, we do not expect source models to transfer well to these tasks.[1] Yet, we still obtain the best accuracy on DMLab, dSpr-Loc, and sNORB-Azimuth.

	Caltech101	CIFAR-100	DTD	Flowers102	Pets	SVHN	Sun397	Natural	Camelyon	EuroSAT	Resisc45	Retinopathy	Specialized	Clevr-Count	Clevr-Dist	DMLab	KITTI-Dist	dSpr-Loc	dSpr-Ori	sNORB-Azim	sNORB-Elev	Structured	Mean
IN+Transfer	88.1	47.0	57.4	85.8	82.8	75.3	27.8	66.3	81.0	95.0	80.0	72.7	82.2	73.1	55.9	43.6	75.7	18.7	58.6	21.2	46.0	**49.1**	**62.4**
DISTILLWEIGHTED	88.6	60.9	62.4	86.1	84.4	79.0	38.4	**71.4**	80.6	95.9	83.3	72.2	**83.0**	57.4	45.6	44.6	67.7	27.4	44.9	23.9	38.2	43.7	62.2
DISTILLNEAREST	88.9	59.5	61.9	86.2	84.5	79.5	37.6	71.1	80.5	95.8	83.2	71.7	82.8	60.5	45.4	45.2	67.9	20.8	40.6	24.2	36.5	42.6	61.6

Table 4: Top-1 accuracy by dataset in VTAB. The accuracy for each task is in grey, and the average accuracy for each category of tasks is in black. Note, the ● *Mean* is the average across all tasks, not categories. The largest value in each column is marked in bold. Here DISTILLWEIGHTED is with $p = 9$.

A.2 Relative accuracy of single-source distillation

Similarly to Table 3, we extend our evaluation of how well the task similarity selects the best source models for single-source distillation. We report the ratio between the average test accuracy of the top-k target models ranked using the task similarity and the average test accuracy for the actual top-k target models found after the fact in Table 5, Table 6, and Table 7 for $k = 1$, $k = 3$, and $k = 5$, respectively.

We find that generally, using task similarity on feature representations rather than the corresponding pseudo-labels yields better rankings, but also that PARC shows very little difference between features and pseudo-labels for all considered $k \in \{1, 3, 5\}$.

Relative accuracy over all k. The relative accuracy measure reported above is sensitive to k and the actual accuracy values of the models. I.e. if a metric flips the order of the best and second best model when there is a notable performance gap between the two models, the relative accuracy for $k = 1$ will be low, and we might be mistaken to believe the metric is not working well. However, the metric might rank every model for $k > 2$ perfectly correct, and since we typically utilize the full set of source models, the initial mistake should not be detrimental to the selection of the task similarity metric. Thus, in Figure 7 we plot the relative accuracy for each task similarity metric and all $k \in \{1, \ldots, S\}$. We find that while PARC on feature representations is outperformed by both PARC and CKA on pseudo-labels for $k < 3$, PARC on feature representations outperforms all the other metrics for $k \geq 3$. In particular, from Table 8 we have that on average over all $k < S$, PARC, performs the best.

---

[1]The ● *Structured* tasks are mainly (ordinal) regression tasks transformed into classification tasks, and thus it seems reasonable to expect very general features (such as those from an ImageNet pre-trained model) to generalize better to such constructed tasks than specialized source models.

		CIFAR-10	CUB200	ChestX	EuroSAT	ISIC	NABird	Oxford Pets	Stanford Dogs	Mean
Pseudo	CKA	**99.6**	**100.0**	**96.1**	99.5	98.1	**100.0**	**100.0**	**100.0**	**99.2**
	PARC	99.3	**100.0**	93.6	99.5	**98.3**	**100.0**	98.4	**100.0**	98.6
	RSA	99.3	74.8	94.8	99.5	**98.3**	86.6	97.8	95.6	93.4
Feature	CKA	**99.6**	81.0	92.6	**99.8**	98.3	**100.0**	**100.0**	**100.0**	96.4
	PARC	**99.6**	**100.0**	94.6	99.5	97.7	**100.0**	95.1	**100.0**	98.3
	RSA	**99.6**	**100.0**	92.6	99.5	**98.3**	80.6	**100.0**	**100.0**	96.3

Table 5: Relative accuracy of top-1 single-source distilled target model selected by task similarity over the best model found in hindsight. We compute the test accuracy of the highest-ranked target model (ranked by some task similarity) and divide this by the test accuracy of the best-performing target model.

		CIFAR-10	CUB200	ChestX	EuroSAT	ISIC	NABird	Oxford Pets	Stanford Dogs	Mean
Pseudo	CKA	99.1	95.6	97.4	99.6	98.8	89.4	**100.0**	97.6	97.2
	PARC	99.5	**100.0**	95.5	99.6	98.5	99.7	98.8	**99.7**	98.9
	RSA	**100.0**	77.7	96.5	99.7	98.5	87.2	98.6	97.6	94.5
Feature	CKA	**100.0**	95.6	97.0	**99.8**	**99.0**	93.3	**100.0**	96.4	97.6
	PARC	**100.0**	**100.0**	**97.8**	99.7	98.3	**100.0**	97.1	98.5	**98.9**
	RSA	**100.0**	**100.0**	96.7	99.8	98.9	94.9	98.9	98.8	98.5

Table 6: (Identical to Table 3) Relative accuracy of top-3 single-source distilled target models selected by task similarity over the average of the 3 best models found in hindsight. We compute the average test accuracy of the top-3 highest ranked target models and divide this average by the average test accuracy of the 3 best-performing target models.

		CIFAR-10	CUB200	ChestX	EuroSAT	ISIC	NABird	Oxford Pets	Stanford Dogs	Mean
Pseudo	CKA	99.3	98.7	**98.3**	99.7	99.0	92.9	99.2	98.4	98.2
	PARC	99.7	**100.0**	96.7	99.7	98.9	94.5	**99.4**	98.4	98.4
	RSA	99.7	83.2	97.6	99.8	99.0	84.9	99.2	92.8	94.5
Feature	CKA	**99.7**	97.4	97.7	99.8	98.9	96.5	99.2	97.8	98.4
	PARC	**99.7**	100.0	97.9	99.8	99.1	**99.7**	97.5	**99.7**	**99.2**
	RSA	**99.7**	99.7	97.9	**99.8**	**99.2**	97.9	98.9	**99.7**	99.1

Table 7: Relative accuracy of top-5 single-source distilled target models selected by task similarity over the average of the 5 best models found in hindsight. We compute the results analogously to Table 6 with $k = 5$.

	CKA	PARC	RSA
Pseudo	0.985	0.990	0.974
Feature	0.986	**0.993**	0.991

Table 8: The mean relative accuracy, across all k, for each metric in Figure 7. The average is bounded in $(0, 1]$, and 1 corresponds to perfect ordering by task similarity. We find that using feature representations consistently outperforms pseudo-labels and that for both feature representations and pseudo-labels PARC performs the best.
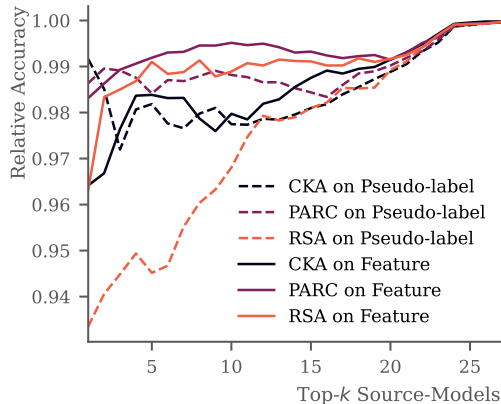
Figure 7: Relative accuracy of top-k single-source distilled target models selected by task similarity over the average of the top-k actual best target models found in hindsight. If the ordering by task similarity were perfectly correct, the relative accuracy would be 1 for all k. See Table 8 for the average of each metric across all k.

	CIFAR-10	CUB200	ChestX	EuroSAT	ISIC	NABird	Oxford Pets	Stanford Dogs	Mean
IN+Transfer	92.4	42.8	47.3	97.4	81.6	37.3	75.9	62.6	67.2
IN+FixMatch	**93.5**	41.9	38.5	**98.1**	**82.6**	42.8	83.4	65.8	68.3
DISTILLEQUAL	90.8	53.5	45.7	97.5	81.5	41.4	82.1	62.1	69.3
DISTILLWEIGHTED(1)	91.1	55.6	46.5	97.9	81.5	42.5	83.3	64.4	70.3
DISTILLWEIGHTED(3)	91.6	57.7	46.5	97.7	82.3	44.5	84.6	67.4	71.6
DISTILLWEIGHTED(6)	91.8	59.0	46.7	97.5	82.5	46.7	**84.7**	69.1	72.3
DISTILLWEIGHTED(9)	92.0	59.6	46.8	97.6	82.4	47.6	84.5	69.5	72.5
DISTILLWEIGHTED(12)	92.0	60.0	**47.7**	97.6	82.2	**48.3**	84.4	69.9	**72.8**
DISTILLWEIGHTED(15)	92.6	**60.3**	46.7	97.5	81.7	48.2	83.9	70.2	72.6
DISTILLNEAREST	92.0	59.6	46.8	97.4	81.0	47.4	81.9	**71.3**	72.2

Table 9: Test accuracy of DISTILLWEIGHTED with various choices of p, compared to the baseline methods of IN+TRANSFER and IN+FIXMATCH. We highlight the largest value for each target task in **bold**, and the results are also visualized in Figure 6.

A.3 Ablation of *p* for DISTILLWEIGHTED

We report the values associated with Figure 6 for each target task and all considered choices of p in Table 9.

A.4 DISTILLWEIGHTED with ResNet-50 as target architecture

In the main part of the article, we consider the computationally constrained setting, where some compute budget restricts the possible size of our target model. Thus, we use MobileNetV3 models as target models throughout the main paper. However, in Table 10 we remove the computational budget and allow the target model to be of any architecture, and particularly we use a ResNet-50 as the target model.

We compare DISTILLWEIGHTED (with $p = 0$ and $p = 12$) initialized with either ImageNet pre-trained weights or the weights of the highest ranked ResNet-50 source model to IN+TRANSFER and FINE-TUNE SELECTED SOURCE. We find that DISTILLWEIGHTED initialized from ImageNet outperforms IN+TRANSFER on average for both equal weighting and $p = 12$, but underperforms FINE-TUNE SELECTED SOURCE for both p. However, since FINE-TUNE SELECTED SOURCE is initialized from well-selected source model weights, the comparison is not entirely fair. Thus, we also consider the case where we initialize the target model for DISTILLWEIGHTED with the weights of

	Model Init.	CIFAR-10	CUB200	ChestX	EuroSAT	ISIC	NABird	Oxford Pets	Stanford Dogs	Mean
IN+Transfer	ImageNet	92.9	42.0	43.4	96.8	79.9	39.9	83.3	65.9	68.0
Fine-tune Source	Source	**93.0**	**70.8**	43.9	97.2	**81.3**	47.4	84.8	**79.3**	**74.7**
DISTILLEQUAL	ImageNet	87.8	57.3	46.1	97.0	78.9	42.4	84.1	64.5	69.8
DISTILLWEIGHTED(12)	ImageNet	91.5	64.5	45.4	97.0	78.9	49.8	**87.1**	74.2	73.6
DISTILLEQUAL	Source	87.5	68.8	45.5	**97.4**	81.2	43.2	81.9	65.1	71.3
DISTILLWEIGHTED(12)	Source	91.6	70.0	**47.6**	97.0	80.8	**50.0**	85.7	73.8	74.6

Table 10: DISTILLWEIGHTED with ResNet-50 as target model architecture. We compare fine-tuning of the highest ranked source model [9] with DISTILLWEIGHTED to both ImageNet-initialized target models and target models initialized from the highest ranked ResNet-50 source model. For $p = 12$, DISTILLWEIGHTED performs on par with fine-tuning the selected source model. The largest value for each target task is in **bold**.

the highest ranked ResNet-50 source model, and find that for $p = 12$ DISTILLWEIGHTED performs on par with FINE-TUNE SELECTED SOURCE.

A.5 Normalization of task similarity for source model weighting

We propose to choose the weights $\boldsymbol{\alpha} = (\alpha_1, \ldots, \alpha_S)$ as

$$\alpha_i = \frac{\underline{e}_i^p}{\sum_{s=1}^S \underline{e}_s^p}, \quad \text{where} \quad \underline{e}_j = \mathbb{1}_{(e_j > 0)} \, e_j$$

for $j = 1, \ldots, S$, and e_s is the task similarity for source model $\mathcal{M}_s$, evaluated on the target task, normalized to satisfy $e_s \in [0, 1]$ with min-max normalization over all e_s. Here, the hyperparameter, p can be used to increase/decrease the relative weight on the highest ranked source models, with the extremes $p = 0$ and $p \to \infty$ corresponding to equal weight and single-source distillation, respectively. An alternative way to obtain our normalization is to use the softmax function on the task similarities,

$$\alpha_i = \frac{\exp\left(\frac{e_i}{T}\right)}{\sum_{s=1}^S \exp\left(\frac{e_s}{T}\right)}.$$

This does not require clipping the task similarity at 0, and with the temperature, T, we can adjust the relative weight on particular source models. Here, large T flattens the weights, and $T \to \infty$ corresponds to an equal weighting of all source models, while small T increases the weight on the highest-ranked source models. Quantitatively, the two normalization methods can yield similar transformations with appropriate choices of p and T - see Figure 8.

A.6 Smaller amount of labeled data

We now repeat the experiment of the main paper across the 8 target datasets with a reduced amount of labeled samples. Here, we reduce the number of labeled samples to 5% (rather than 20%) of the training set and report the accuracy in Table 11. We find a similar pattern as observed in the main experiment, where DISTILLWEIGHTED distillation on average outperforms IN+TRANSFER irrespective of the choice of p. For $p = 9$ DISTILLWEIGHTED outperforms IN+TRANSFER by 6.8%-point on average and in particular 15.5%-points on CUB200, whereas the only loss in performance is on ChestX with a drop of 0.9%-point.

A.7 Different Measures of Correlation

In order to evaluate the quality of a task similarity metric to estimate the performance of a target model after distillation, we consider the correlation between the computed metric and the actual observed performance after distillation. However, since we have no reason to believe that the relationship is linear, we consider the Spearman correlation in the main paper. However, for completeness of
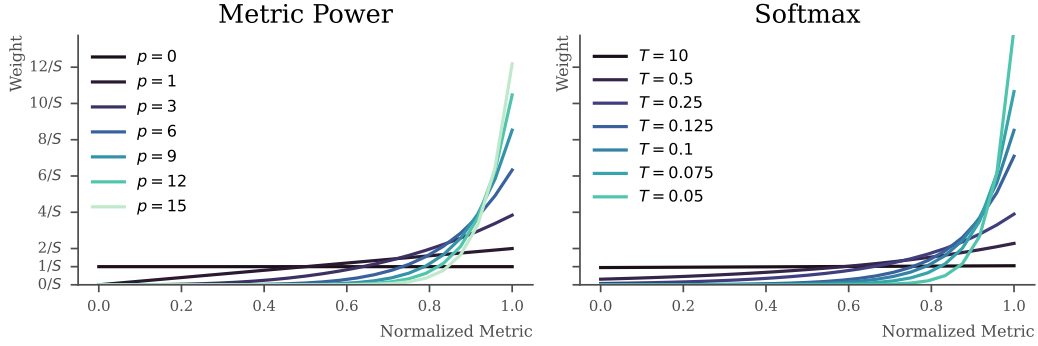
Figure 8: Transformation of weights for various choices of power (left) or softmax temperature (right). Here S is the number of source models, and we consider equidistantly distributed normalized metrics.

	CIFAR-10	CUB200	ChestX	EuroSAT	ISIC	NABird	Oxford Pets	Stanford Dogs	Mean
IN+Transfer	88.0	16.8	**43.5**	94.8	73.9	14.4	55.0	38.9	53.2
DISTILLWEIGHTED(1)	88.1	29.2	42.3	**95.9**	76.3	20.5	66.6	42.1	57.6
DISTILLWEIGHTED(9)	**90.2**	**32.3**	42.6	95.9	**76.7**	**24.8**	**68.2**	49.0	**60.0**
DISTILLNEAREST	87.2	31.4	39.7	95.1	75.4	24.0	58.9	**49.7**	57.7

Table 11: Distillation on the eight target tasks with only 5% labeled samples per task. Again, we compare to the baseline of IN+TRANSFER. The largest value for each target task is in **bold**.

exposition, we report Pearson correlation and Kendall's Tau in Table 12 and Table 13, respectively. For both these correlation measures, the overall conclusions are the same: Using feature representations is preferable to pseudo-labels, and PARC generally outperforms both CKA and RSA, albeit not by much over CKA.

		CIFAR-10	CUB200	ChestX	EuroSAT	ISIC	NABird	Oxford Pets	Stanford Dogs	Mean
Pseudo	CKA	0.62	**0.85**	0.07	0.30	-0.06	0.33	0.67	0.21	0.37
	PARC	0.75	0.74	-0.03	0.27	-0.00	0.36	0.63	0.51	0.40
	RSA	0.75	0.13	-0.07	0.38	0.04	-0.09	0.66	0.40	0.27
Feature	CKA	0.84	0.60	**0.39**	0.29	0.00	0.30	0.71	0.54	0.46
	PARC	0.86	0.73	0.17	**0.46**	-0.06	**0.58**	0.77	0.78	**0.54**
	RSA	**0.90**	0.85	0.07	0.45	**0.04**	0.27	**0.87**	**0.83**	0.54

Table 12: Pearson correlation between test accuracy after all possible single-source distillations and task similarity associated with the source models. Similar to Table 2.

A.8 Choice of Task Similarity Metrics

Recently, multiple measures intended to estimate the transferability of a source model have been proposed. However, despite the very recently published Multi-Source Leep (MS-LEEP) and Ensemble Leep (E-Leep) no task similarity metric considers the estimation over multiple models at once [4]. Thus, we consider each source model separately and compute the metrics independent of other source models. This has the added benefit of reducing the number of metric computations required as we do

	CIFAR-10	CUB200	ChestX	EuroSAT	ISIC	NABird	Oxford Pets	Stanford Dogs	Mean
Pseudo CKA	0.51	0.46	0.16	0.28	-0.05	0.24	0.49	0.07	0.27
PARC	0.61	0.64	0.01	0.12	0.02	0.36	0.54	0.39	0.34
RSA	0.62	0.17	-0.07	0.22	**0.08**	-0.01	0.48	0.29	0.22
Feature CKA	0.67	0.34	**0.25**	0.14	-0.05	0.40	0.50	0.38	0.33
PARC	0.69	**0.67**	0.14	**0.31**	-0.10	**0.65**	0.62	0.67	**0.46**
RSA	**0.72**	0.65	0.02	0.28	0.02	0.19	**0.72**	**0.67**	0.41

Table 13: Kendall Tau correlation between test accuracy after all possible single-source distillations and task similarity associated with the source models. Similar to Table 2.

not need to compute the task similarity for all possible combinations of n models from S possible (i.e. $\binom{n}{S}$), which grows fast with S.

Assume $\mathbf{X} \in \mathbb{R}^{N \times d_X}$ and $\mathbf{Y} \in \mathbb{R}^{N \times d_Y}$, and that $\mathbf{K}_{ij} = k(\mathbf{x}_i, \mathbf{x}_j)$ for and $\mathbf{L}_{ij} = l(\mathbf{y}_i, \mathbf{y}_j)$ where k, and l are two (similarity) kernels as well as $\mathbf{x}_i, \mathbf{x}_j$ and $\mathbf{y}_i, \mathbf{y}_j$ are rows of $\mathbf{X}$ and $\mathbf{Y}$, respectively. Then we have that CKA is defined as

$$\rho_{\mathrm{CKA}}(\mathbf{X}, \mathbf{Y}) \stackrel{\mathsf{def}}{=} \frac{\mathrm{HSIC}(\mathbf{K}, \mathbf{L})}{\sqrt{\mathrm{HSIC}(\mathbf{K}, \mathbf{K})\mathrm{HSIC}(\mathbf{L}, \mathbf{L})}},$$

where $\mathbf{K}, \mathbf{L} \in \mathbb{R}^{N \times N}$ and HSIC is the Hilbert-Schmidt Independence Criterion,

$$\mathrm{HSIC}(\mathbf{K}, \mathbf{L}) \stackrel{\mathsf{def}}{=} \frac{1}{(N-1)^2} \mathrm{tr}\left(\mathbf{K}\mathbf{H}_N\mathbf{L}\mathbf{H}_N\right), \quad \text{with}$$

$$\mathbf{H}_N \stackrel{\mathsf{def}}{=} \mathbf{I}_N - \frac{1}{N}\mathbf{1}\mathbf{1}^{\mathsf{T}}.$$

In particular, if both k and l are linear kernels, then

$$\rho_{\mathrm{CKA}}(\mathbf{X}, \mathbf{Y}) = \frac{\|\mathbf{Y}^{\mathsf{T}}\mathbf{X}\|_F^2}{\|\mathbf{X}^{\mathsf{T}}\mathbf{X}\|_F \|\mathbf{Y}^{\mathsf{T}}\mathbf{Y}\|_F},$$

where $\|\cdot\|_F$ is the Frobenius norm. We use the linear kernel throughout this paper and refer to Cortes et al. [12] for additional details on CKA.

For RSA, we consider the dissimilarity matrices given by

$$\mathbf{K}_{ij} \stackrel{\mathsf{def}}{=} 1 - \mathrm{pearson}(\mathbf{x}_i, \mathbf{x}_j) \quad \text{and}$$

$$\mathbf{L}_{ij} \stackrel{\mathsf{def}}{=} 1 - \mathrm{pearson}(\mathbf{y}_i, \mathbf{y}_j),$$

where $\mathbf{X}$ and $\mathbf{Y}$ are assumed normalized to have mean 0 and variance 1. We then compute RSA as the Spearman correlation between the lower triangles of $\mathbf{K}$ and $\mathbf{L}$,

$$\rho_{\mathrm{RSA}}(\mathbf{X}, \mathbf{Y}) \stackrel{\mathsf{def}}{=} \mathrm{spearman}\left(\{\mathbf{K}_{ij} \mid i < j\}, \{\mathbf{L}_{ij} \mid i < j\}\right).$$

For additional details on RSA, we refer the reader to Dwivedi and Roig [14]. While Bolya et al. [9] introduces PARC alongside a heuristic and feature reduction, the PARC metric is almost identical to RSA. However, RSA was introduced to compute similarities between two sets of representations, and PARC was aimed at computing similarities between a set of representations and a set of labels associated with the dataset. Thus, in our use of PARC, it merely differs from RSA in the lack of normalization of $\mathbf{Y}$, which is assumed to be one-hot encoded vectors of class labels from the probe dataset.

B Experimental Details

In the following, we provide some experimental details.

B.1 Main Experiments

Unless otherwise mentioned, we use SGD with a learning rate of 0.01, weight decay of 0.0001, batch size of 128, and loss weighting of $\lambda = 0.8$. We initialize our target models with the ImageNet pre-trained weights available in torchvision (https://pytorch.org/vision/stable/models) and consider 28 fine-tuned models from Bolya et al. [9] publicly available at github.com/dbolya/parc as our set of source models. The source models consist of each of the architectures (AlexNet, GoogLeNet, ResNet-18, and ResNet-50) trained on CIFAR-10, Caltech101, CUB200, NABird, Oxford Pets, Stanford Dogs, and VOC2007. Note, we always exclude any source model trained on the particular target task, thus effectively reducing the number of source models for some target tasks. For FixMatch we use a batch size of 128 (with a 1:1 ratio of labeled to unlabeled samples for each batch) and fix the confidence threshold at 0.95 and the temperature at 1. We keep the loss weighting between the supervised loss and the unlabeled FixMatch loss at $\lambda = 0.8$.

B.2 VTAB Experiments

For each VTAB experiment, we consider the full training set (as introduced in Zhai et al. [46]) as the unlabeled set, $\mathcal{D}_\tau^u$, and the VTAB-1K subset as the labeled set, $\mathcal{D}_\tau^l$. We use the Pytorch implementation from Jia et al. [21] available at github.com/KMnP/vpt.

We use SGD with a learning rate of 0.005, weight decay of 0.0001, batch size of 128 equally split in 64 labeled and unlabeled samples, and loss weighting of $\lambda = 0.9$. We train our models for 100 epochs, where we define one epoch as the number of steps required to traverse the set of unlabeled target data, $\mathcal{D}_\tau^u$ when using semi-supervised methods, or merely as the number of steps to traverse the labeled set, $\mathcal{D}_\tau^l$, for supervised transfer methods. We initialize our target models with the BiT-M ResNet-50x1 model fine-tuned on ILSVRC-2012 from BiT [22] publicly available at github.com/google-research/big_transfer.

We consider the 19 BiT-M ResNet-50x1 models fine-tuned on the VTAB-1K target tasks from Kolesnikov et al. [22] as the set of source models. We always exclude the source model associated with the target task from the set of source models, and thus effectively have 18 source models available for each target task in VTAB. We use the PARC metric on the source model features to compute the source weighting, but also only use the top-5 highest-ranked source models to reduce the computational costs of training. Furthermore, we use $p = 9$ for DISTILLWEIGHTED.

C Domain gap between source tasks, targets tasks and ImageNet

As is evident from Figure 4 and Table 1, both DISTILLNEAREST and DISTILLWEIGHTED do not yield notable improvements on e.g. ChestX and ISIC, but yield significant improvements on e.g. CUB200 and Oxford Pets. Notably, for the latter target tasks there are semantically similar source tasks present in our set of source models, while this is not true for the former target tasks. Hence, as one would expect, the availability of a source model trained on source tasks similar to the target tasks is important for cross-domain distillation to work well, which is expected to be true for both DISTILLNEAREST and DISTILLWEIGHTED. Indeed, the task similarity metrics considered in this paper all aim at measuring alignment between tasks, and if the alignment between source and target tasks is small, we do not expect to gain much from distillation. This is affirmed by our experiments in *e.g.* Table 1.

C.1 A note on potential data overlap between source and target tasks

Whenever any type of transfer learning is applied, including using ImageNet initializations, we (often implicitly) assume that the model we transfer from has not been trained on any data from the target test set. Although this assumption is often satisfied in practice due to domain gaps between the source and target task, utilizing initializations trained on e.g. ImageNet can potentially violate the assumption. This is due to the fact that ImageNet and many other modern publicly available datasets are gathered from various public websites and overlaps between samples in different datasets might occur.

Thus, it is natural to question whether the observed improvements are due to methodological advances or information leakage between source and target tasks. To ensure our advancements are valid we

carefully remove any source model associated with the target task from the set of source models, $\mathcal{S}$. However, information leakage might still appear if *e.g.* there are identical samples in the target dataset and the source dataset or ImageNet. Despite large overlaps being improbable, it has been shown that there e.g. is a minor overlap (of at least 43 samples) between the training set of ImageNet and the test set of CUB200 (see e.g. https://gist.github.com/arunmallya/a6889f151483dcb348fa70523cb4f578). However, since the test set of CUB200 consists of 5794 samples, the presence of such a minor overlap should not affect the true performance of a model much.

In our experiments, we consistently compare our target models (initialized with ImageNet weights) to either identically initialized target models or source models initialized with either ImageNet weights or with weights from a source task. Hence, any potential gain from information leakage between ImageNet and a target task would bias both our results and the baselines, and thereby not affect our overall results. Furthermore, while an overlap between a source and target task might unfairly benefit the performance of our methods compared to IN+TRANSFER and IN+FIXMATCH, such an overlap would likely benefit the fine-tuned source models even more making this baseline even harder to outperform (see e.g. Figure 2 and Table 1). Thus, our results should be at most as biased as the baselines.